Efficient Red Emission from Europium Chelate-Silicone Host-Guest Hybrids

Thanh H. Tran[a], Michael Bentlage[a], Marina M. Lezhnina[b], and Ulrich Kynast[a]

[a] Münster University of Applied Sciences, Department of Chemical Engineering, Stegerwaldstraße 39, 48565 Steinfurt, Germany

[b] On leave from Volga State University of Technology, Department of Physics, Lenin-pl.3, Yoshkar-Ola, 424000, Russia

Reprint requests to Prof. Dr. U. Kynast. Fax: +49(0)2551-962119. E-mail: uk@fh-muenster.de

Z. Naturforsch. **2014**, *69b*, 210 – 216 / DOI: 10.5560/ZNB.2014-3278
Received October 2013

Due to their ease of fabrication, chemical stability and optical transparency polydimethylsiloxane-derived silicones ($[O\text{-}Si(CH_3)_2]_\infty$) are excellent matrices to enable optical functions. We here report on the luminescence of silicone hybrids with red-emitting europium diketonate complexes, which have not been described previously in this matrix. The problem of too low solubility of the pure complexes has been resolved by co-coordination with trioctylphosphine oxide (TOPO), which permits complex concentrations of up to 5×10^{-3} mol L^{-1}, at the same time maintaining complete transparency. Quantum efficiencies in excess of 60 % could thus be obtained for benzoyltrifluoroacetonates, and near 50 % for thenoyltrifluoroacetonates. These high efficiencies have been confirmed by room-temperature life time measurements, which displayed straight single-exponential decay behavior for both complexes independent of their concentration in the silicone.

Key words: Eu Chelates, Silicone, Luminescence, Hybrid

Introduction

Silicones obtained from condensation crosslinking of polydimethylsiloxane (PDMS) with, *e. g.*, tetraethyl orthosilicate (TEOS) are completely colorless, slightly flexible polymers. Typically, the precursors PDMS, TEOS and a catalyst like DBTL (dibutyltin dilaurate) are moulded into a desired shape or spun to give corresponding layers.

Luminescence activation of the silicones can be realized by several methods, among which dissolving luminophores in the precursor mixture to give solid solutions after curing, occasionally referred to as host-guest polymers, is probably the most feasible and easy-to-perform task. Numerous dyes have been imbedded into silicone matrices, among them rhodamines, coumarines, perylene derivatives, phthalocyanines, and porphyrins, for mere optical "show" effects and luminescent marking, but also in luminescent solar cell concentrators [1] and oxygen [2 – 10], CO_2 [5, 11, 12] and SO_2 [13] sensing in particular. However, due to the comparably small Stokes shifts of the embedded organic dyes, most of the silicone materials will assume a body color, unless their absorption is in the UV, which on the other hand, restricts the dye emission to the blue spectral range. This unfavorable situation can be circumvented by using metalorganic complexes replacing the purely organic dyes.

It is well known that rare-earth ions display very large apparent Stokes shifts on excitation of higher *f* states due to the internal relaxation process leading to predominant emission from usually only one characteristic excited state (see *e. g.* refs. [14, 15]). This excited state is, in the case of Eu^{3+}, located at approximately 17 200 cm^{-1} ($^5D_0$) above the ground state ($^7F_0$), *i. e.* in the red-orange spectral range, and at approximately 20 500 cm^{-1} ($^5D_4$) above the ground state ($^7F_6$) in the case of the Tb^{3+} ion. Due to spin-orbit coupling, both ions possess a manifold of six further states in close energetic proximity to the ground state, such that the radiative return from the excited Eu^{3+} ($^5D_0$) and Tb^{3+} ($^5D_4$) states, respectively, can proceed into either one of the altogether seven states. The probability of return to either of these is governed by

quantum mechanical selection rules, resulting in a predominant ("hypersensitive") red emission at approximately 612 nm ($^5D_0 \rightarrow {}^7F_2$) for Eu^{3+} (if the Eu^{3+} coordination sphere is non-centrosymmetric), and the strongest, green emission at 545 nm ($^5D_4 \rightarrow {}^7F_5$) for Tb^{3+} [16, 17].

To overcome the weak absorption strength for parity and spin-forbidden $f-f$ transitions in rare-arth ions, ligation with strongly absorbing organic moieties and the "antenna" effect are now heavily exploited, *e. g.* in β-diketonate and carboxylate complexes [18–22], to grant sufficient excitability and the narrow and long-lived line emission of Eu^{3+} and Tb^{3+}. In the context of silicon polymer embeddings yet another bottleneck has to be resolved, because the essentially non-polar silicone matrix does not dissolve satisfying amounts of the mentioned complexes, which is especially true for simple but highly efficient aryl carboxylates. Recently, we were able to successfully tackle the solubility problem by introducing trioctylphosphine oxide (TOPO) as a co-ligand to Tb(salicylate)$_3$, "Tb(sal)$_3$(TOPO)$_2$" [23], which affords an efficiently green emitting hybrid with the silicone matrix [24]; a similar approach of co-coordination had previously been reported for perfluorinated diketonates in polymethylmethacrylate (PMMA) [25]. Pure diketonates of Tb and Eu in PMMA matrices have also been described recently [26], in which, additionally, a new intermolecular energy transfer was identified. Other common polymer matrices which have previously been functionalized with rare-earth complexes to give transparent hybrids, include, *e. g.* epoxy-resins, polycarbonates, polyurethanes and polyvinyl pyrrolidones [27–32], while surprisingly few reports on silicones as hosts to europium complexes have appeared [33–35], neither of them elaborating on conventional diketonates.

Similar to the case of Tb^{3+}, red line emitting silicone hybrids can also be obtained by co-coordination of TOPO to thenoyltrifluoroacetonates (ttfa) and benzoyltrifluoroacetonates (btfa) of Eu^{3+} (see Fig. 1 for sketches of the ligands), as will be shown below. In general, rare-earth ions (*Ln*) in complexes of similar compositions (*Ln*(ttfa)$_3$(TPPO)$_2$, *Ln*(btfa)$_3$(TPPO)$_2$, TPPO = triphenylphospine oxide) adopt a distorted, trigonal-dodecahedral (approximate D_{2d} symmetry) or square-antiprismatic coordination (approximately D_{4d}) of the ligand and co-ligand oxygen atoms [36–38].

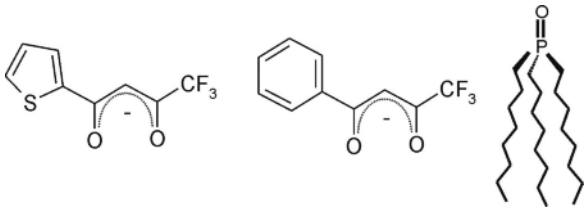

Fig. 1. Sketches of the ligands used in this investigation: thenoyltrifluoroacetonate (ttfa, left), benzoyltrifluoroacetonate (btfa, center) and trioctylphosphine oxide (TOPO, right).

Unfortunately, we could not find a blue rare-earth emitter of sufficient efficiency to complement the red- and green-emitting complexes; neither the emission of the Tm^{3+} ion in diketonate complexes nor the broad-band blue ligand emission (phosphorescence or fluorescence) of the salicylate ion in Na, La, Gd, or Y salicylates proved to be useful in the silicone matrix.

Experimental Section

Preparation of the chelate complexes Eu(btfa)$_3$(TOPO)$_2$ and Eu(ttfa)$_3$(TOPO)$_2$

The Eu chelates were prepared as described in [39] using $Eu(NO_3)_3(H_2O)_6$ which was consecutively co-coordinated with btfaH or ttfaH by dissolving the components in CH_3CN, followed by addition of 2 aliquots of TOPO, evaporation of the solvents and washing the residue with small amounts of hexane. The compositions of all new complexes were verified by elemental analysis and IR spectroscopy, the IR spectra obviously consisting of a wealth of absorption bands. We therefore focus on relevant, strong C=C and C=O absorptions of the diketo-fragment following recent assignments of Sc(acetylacetonate)$_3$ [40] and Sm(tetramethylheptanedionate)$_3$ [41] vibrations, and the P=O vibration by comparing with free TOPO, where applicable (Table 1).

The Eu^{3+} content was determined by complexometric titration with Na_2EDTA (from Merck) using xylenol orange as indicator. Carbon analyses were carried out using an Eltra CS 800 carbon and sulfur determinator.

Preparation of the chelate-silicone hybrids

The TOPO-co-coordinated complexes were converted into the silicone hybrids by a preparation essentially following the procedures previously described for Tb(sal)$_3$(TOPO)$_2$ (*i. e.* polydimethylsiloxane with an average molecular weight (M_n) of 26 000 g mol^{-1}, tetraethylorthosilicate, acetone as a dilutand, dibutyltin laurate as catalysts) [24], except that the desired amounts of

Table 1. Selected IR data and analytical results for the complexes used[a].

		$Eu(btfa)_3(H_2O)_2$	$Eu(btfa)_3(TOPO)_2$	$Eu(ttfa)_3(H_2O)_2$[b]	$Eu(ttfa)_3(TOPO)_2$
		IR vibrational frequencies (cm^{-1})			
ν(C=O)		1613	1627	1604	1617
ν(C=C), ν(C=O)		1576	1581		
ν(C=C), δ(C=CH)		1533	1532	1543	1535
ν(C=O)		1491	1488	1411	1416
ν(C=O)		1292	1290	1303	1302
ν(C=O), δ(C=CH)		1188	1182	1192	1181
ν(P=O)		1144	1138	1147	1142
		Elemental analyses (%)[b]			
Eu^{3+}	theor.	18.17	9.66	–	9.5
	exp.	18.02	9.93	–	9.8
Carbon	theor.	43.08	59.53	–	54.3
	exp.	42.86	58.76	–	55.0

[a] Complete IR spectra will be provided by the authors on request; [b] $Eu(ttfa)_3(H_2O)_2$ has been the subject of numerous previous investigations; see, *e. g.* ref. [26]; the IR spectra reproduced there were in complete agreement with our material.

$Eu(btfa)_3(TOPO)_2$, or $Eu(ttfa)_3(TOPO)_2$, respectively, were used. For subsequent optical measurements the non-polymerized mixtures were poured into disposable polystyrene cuvettes (1 cm, Brand Germany, UV-Küvette Plastibrand) or into a self-made, ring-shaped mould of approximately 3 mm in depth and 30 mm in diameter. After curing, the polymer hybrid was removed from the mould to yield free standing and transparent disks of 2.4 to 3.0 mm thickness (measured and checked for plane parallelity with a micrometer screw, see also Fig. 5).

Optical measurements

Absorption, excitation and emission spectra were obtained as described [24] on the silicone disks in transmission using a 500 nm long pass filter, excitation *via* an Acton Monochromator of 300 nm focal length, a 450 W Xe lamp, and an Ocean Optics HR4000 UV/Vis spectrometer. All disk absorption and luminescence measurements were crosschecked in cuvettes as well. The measurements of the disks in the high-concentration range between 4×10^{-4} and 5×10^{-3} mol L^{-1} suffered from a relative imprecision of roughly $\pm 6\,\%$ due to very strong absorption near the irradiated faces of the disks, resulting in a penetration depth-dependent loss of emitted light to the edges of the disks. Due to geometrical constraints this error could not be accounted for in, *e. g.*, an integrating sphere. However, the monoexponential decay curves (see Fig. 4) with almost constant lifetimes (668 to 694 μs for $Eu(ttfa)_3(TOPO)_2$; 726 to 707 μs for $Eu(btfa)_3(TOPO)_2$) over the mentioned concentration range, unambiguously showed the constant quantum yield of all samples. Quantum yield determinations were conducted relative to $Eu(ttfa)_3(phen)$ (phen = 1,10-phenanthroline), which is known to possess a quantum yield of 37 % in CH_3CN (10^{-3} mol L^{-1}) [42]. The concentrations used for the silicone hybrids were in excess of 10^{-3} mol L^{-1}, with less than 0.1 % of the incident intensity being lost to transmission; for the calculations the index of refraction of the silicone matrix was set to 1.5. Luminescence decay times were measured with an Edinburgh Instruments FL 920 lifetime spectrometer (single-photon counting) equipped with an Edinburgh Instruments μF900 flash lamp and a Hamamatsu extended red sensitivity photomultiplier tube.

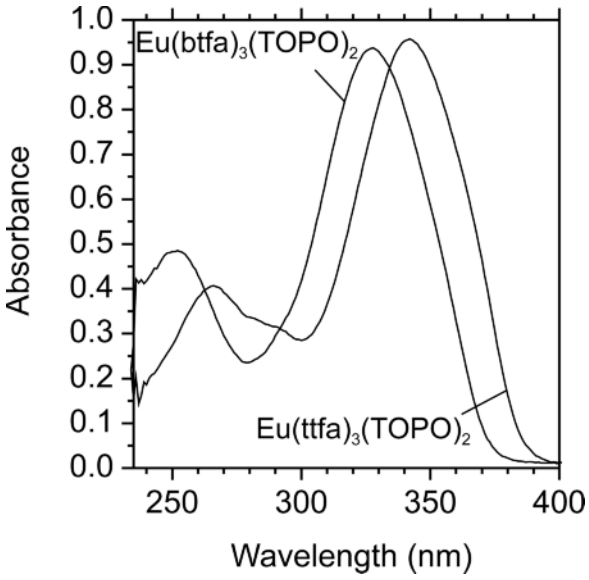

Fig. 2. Absorption spectra of the individual luminophores $Eu(ttfa)_3(TOPO)_2$ and $Eu(btfa)_3(TOPO)_2$ at 2×10^{-5} mol L^{-1} in silicone matrix (1 cm cuvettes). Absorption data are also reproduced in Table 1.

Results and Discussion

Absorption spectra of the individual luminophores $Eu(ttfa)_3(TOPO)_2$ and $Eu(btfa)_3(TOPO)_2$ in silicone matrix are depicted in Fig. 2. The maximum extinction coefficients ε_{max}, the ε_{360} values at 360 nm and the corresponding quantum yields for the 360 nm excitation are summarized in Table 2. $Eu(ttfa)_3(phen)$, usually a good choice for efficient emission, proved to be unsuitable for this investigation, as a too low solubility in the silicone after evaporation of assisting acetone and consecutive curing caused undesired turbidities. As opposed to that, the employment of co-ligating TOPO yielded perfectly transparent materials. It should be pointed out that the quantum yields of the Eu complexes given in Table 2 do not represent the highest values, as the 360 nm excitation chosen for comparable absorptivities of complexes does not correspond to their excitation maxima (see Fig. 3).

Complex	$\lambda_{exc,max}$ (nm)	ε_{max} ($L\,mol^{-1}\,cm^{-1}$)	$\varepsilon_{360\,nm}$ ($L\,mol^{-1}\,cm^{-1}$)	Θ (%)
$Eu(ttfa)_3(phen)$[a]	341	52 000	36 300	37
$Eu(ttfa)_3(TOPO)_2$	342	48 000	35 600	48
$Eu(btfa)_3(TOPO)_2$	330	47 000	16 400	62
$Tb(salicylate)_3(TOPO)_2$[b]	330	10 900	–	67

Table 2. Optical data of the individual luminophors from silicone hybrids. Absorption data from cuvette measurements at 2×10^{-5} mol L^{-1}; quantum yields from disks of thickness 2.4 – 3.0 mm, transmittance < 0.1 %.

[a] In CH_3CN; used as the quantum efficiency reference at 10^{-3} mol L^{-1} [42]; in silicones with $c[Eu(ttfa)_3(phen)] < 7 \times 10^{-5}$ mol L^{-1}, ε became non-constant (increased); [b] ref. [24], excitation at 330 nm.

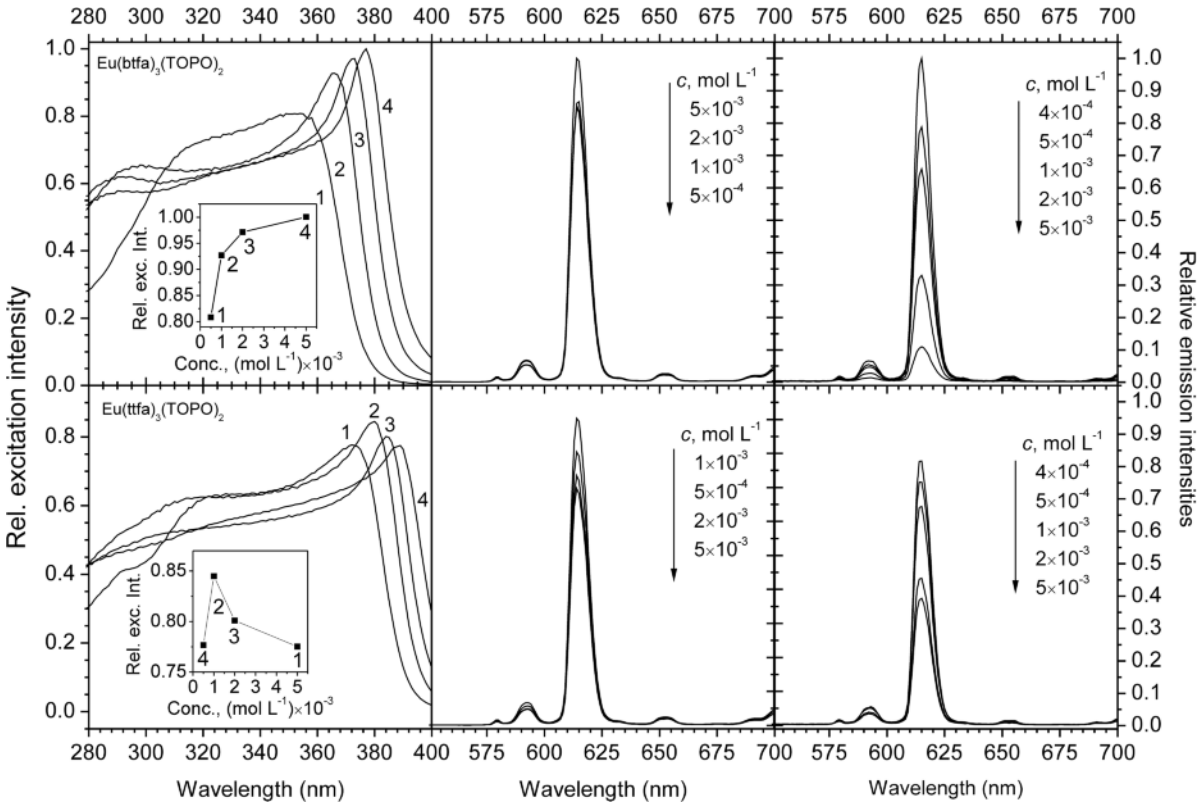

Fig. 3. Excitation and emission spectra of the hybrid samples with varying complex content. The excitation of fabricated disks (left column) was monitored at 615 nm, corresponding emissions of the disks (middle column) and cuvettes (right column) were excited at 360 nm. Top row: $Eu(btfa)_3(TOPO)_2$, bottom row: $Eu(btfa)_3(TOPO)_2$. For clarity, the insets in the left column depict the course of maximum excitation as a function of concentration. For differences in the emission spectra, see text.

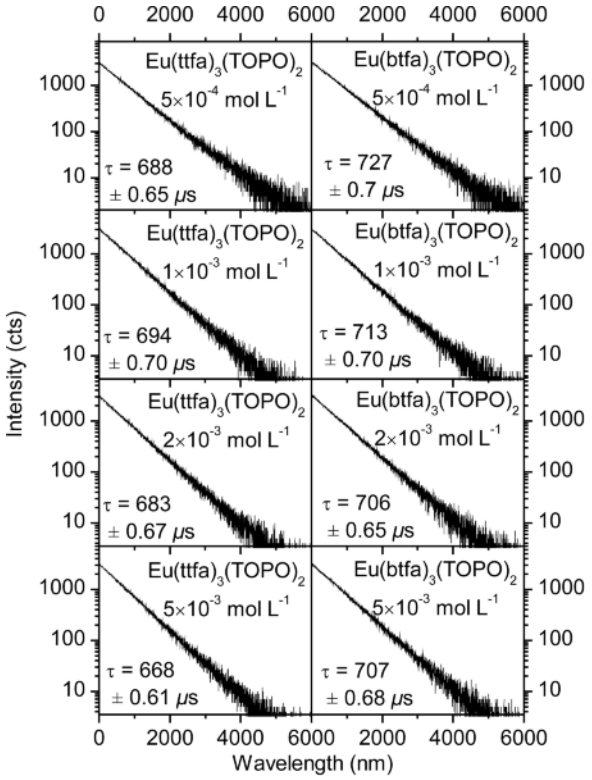

Fig. 4. Lifetimes of the hybrid samples with varying complex concentrations. The single exponential decay character and practically constant decay times should be noted.

Furthermore, the emission intensities do not correlate linearly with the complex concentrations for a twofold reason: on increasing the complex concentration the excitation maxima for the 612 nm-emission experience a blueshift for both complexes, the $Eu(ttfa)_3(TOPO)_2$ eventually being spectrally located at 391 nm, at the same time losing intensity, while $Eu(btfa)_3(TOPO)_2$ only drifts to 377 nm but is accompanied by an intensity gain, as shown in the insets of Fig. 3. The total absorption does not increase linearly, because all incident radiation is practically absorbed (*e. g.* transmission $T_{360} = (1\text{-Absorption}) \approx 0$ for $Eu(ttfa)_3(TOPO)_2$ and $\approx 0.03\,\%$ for $Eu(btfa)_3(TOPO)_2$). The observed redshift of the excitation band (at unchanged absorption maxima) needs some consideration. As mentioned above, $Eu(ttfa)_3(phen)$ showed a lower solubility in the silicone polymer, which leads to visible turbidity at the concentrations used for TOPO-co-coordinated complexes, the latter staying clear up to 5×10^{-3} mol L^{-1}.

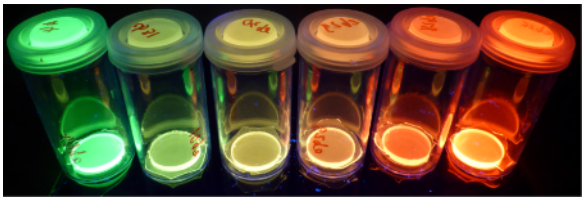

Fig. 5 (color online). Photographic image of the disks for a series of mixed hybrid samples with varying ratios of $Tb(sal)_3(TOPO)_2$ to $Eu(btfa)_3(TOPO)_2$. The samples were obtained by adding increasing amounts of $Eu(btfa)_3(TOPO)_2$ to a 2×10^{-3} mol L^{-1} stock solution of $Tb(sal)_3(TOPO)_2$ (additions from left to right: 0, 1×10^{-4}, 2×10^{-4}, 3×10^{-4}, 4×10^{-4}, 5×10^{-4} mol L^{-1} of $Eu(btfa)_3(TOPO)_2$).

This behavior is indicative of a tendency of the complexes to form aggregates in the matrix. It is most likely that such aggregates form at lower concentrations already, albeit the size of the aggregates obviously remains below the scattering threshold for visible and near UV light.

We have recently been able to demonstrate the aggregation of $Tb(sal)_3(TOPO)_2$ in the same matrix [43]. The exact nature of the interaction between the complexes is unclear at present, however, we speculate that micelle-like aggregates form, in which the alkyl chains of the TOPO molecules are oriented towards the surrounding silicone. The shift of ligand-centered excitation bands may then reflect intermolecular interactions, *e. g.* of the π-stacking or other π-interaction types [44], giving rise to intermediate states between the original LMCT and the ligand triplet state. Lifetime measurements of $Eu(ttfa)_3(TOPO)_2$ and $Eu(btfa)_3(TOPO)_2$ (Fig. 4) are in agreement with this view, as the intermediate states are not expected to lead to any quenching. Correspondingly, the Eu^{3+} decay times, as exhibited by the long-lived $^5D_0$ level ($^7F_2 \leftarrow {}^5D_0$ transition), are unaffected by the aggregation, and furthermore, show no dependence on concentration.

Finally, we would like to mention that the existence of red- and green-emitting, silicone-soluble complexes obviously opens the path to cover all intermediate colors of the red to green range by simply mixing *e. g.* $Eu(btfa)_3(TOPO)_2$ and $Tb(sal)_3(TOPO)_2$ in appropriate ratios (see, *e. g.*, Fig. 5). However, the color prediction turned out to be somewhat complicated, due to a number of intermolecular energy transfers, involving both, ligand-to-ligand and Tb^{3+} to Eu^{3+} transfers, which we are currently trying to unravel. Also in this

context, the mentioned lack of a blue rare-earth emitter is most deplorable, as it presently blocks the access to a wider color gamut. An exit away from this bottleneck may be provided by the use of blue-emitting organic dyes such as Coumarin 460, for which various energy transfers were found. The evaluation of the results is beyond the scope of this article.

Conclusion

Despite the fact that silicones are of high interest for photophysical investigations and applications due to their optical and chemical properties, such as high transparency and chemical stability, and last but not least ready accessibility, very little attention has been devoted to their use as hosts for efficient Eu^{3+} emission in the past. The high quantum yields in excess of 50 % and fairly high concentration levels of up to 5×10^{-3} mol L^{-1}, enabled by the co-ligation with TOPO, provides these new host-guest hybrids with valuable potential in numerous UV conversion devices and luminescent markers. Complementing the red-emitting hybrids with corresponding green Tb^{3+} complexes gives access to the red to green color range. However, an efficient blue rare-earth component for access to a more complete color gamut is not in sight and may instead have to be substituted by suitable organic dyes.

Acknowledgement

H. T. T., M. L. and M. B. gratefully acknowledge funding by the German Ministry of Economics and Technology (ZIM-KF2171201FK9).

[1] M. Buffa, S. Carturan, M. G. Debije, A. Quaranta, G. Maggioni, *Sol. Energy Mater. Sol. Cells* **2012**, *103*, 114 – 118.
[2] W. Barnikol, O. Burkhard, US4775514A, **1988**.
[3] I. Klimant, O. S. Wolfbeis, *Anal. Chem.* **1995**, *67*, 3160 – 3166.
[4] H. Trubel, W. K. R. Barnikol, *Biomed. Tech.* **1998**, *43*, 302 – 309.
[5] G. Liebsch, I. Klimant, B. Frank, G. Holst, O. S. Wolfbeis, *Appl. Spectrosc.* **2000**, *54*, 548 – 559.
[6] F. G. Gao, J. M. Fay, G. Mathew, A. S. Jeevarajan, M. M. Anderson, *J. Biomed. Opt.* **2005**, *10*, 054005/054001 – 054005/054006.
[7] B. J. Basu, *Sens. Actuators, B* **2007**, *123*, 568 – 577.
[8] R. Ambekar, P. Jongwon, D. B. Henthorn, K. Chang-Soo, *IEEE Sens. J.* **2009**, *9*, 169 – 175.
[9] J. Lopez-Gejo, D. Haigh, G. Orellana, *Langmuir* **2009**, *26*, 2144 – 2150.
[10] F. Manjón, M. Santana-Magaña, D. García-Fresnadillo, G. Orellana, *Photochem. Photobiol. Sci.* **2010**, *9*, 838 – 845.
[11] O. S. Wolfbeis, B. Kovacs, K. Goswami, S. M. Klainer, *Microchim. Acta* **1998**, *129*, 181 – 188.
[12] M. D. Marazuela, M. C. Moreno-Bondi, G. Orellana, *Appl. Spectrosc.* **1998**, *52*, 1314 – 1320.
[13] T. M. A. Razek, M. J. Miller, S. S. M. Hassan, M. A. Arnold, *Talanta* **1999**, *50*, 491 – 498.
[14] J.-C. Bünzli, S. Eliseeva in *Lanthanide Luminescence: Photophysical, Analytical and Biological Aspects,* Springer Series on Fluorescence, Vol. 7 (Eds.: H. Hänninen, H. Härma), Springer, Berlin Heidelberg, **2011**, pp. 1 – 45.
[15] M. H. V. Werts, *Sci. Prog.* **2005**, *88*, 101 – 131.
[16] G. Blasse, B. C. Grabmaier, *Luminescent Materials*, Springer, Berlin, Heidelberg, **1994**, pp. 33 – 70.
[17] G. H. Dieke, H. M. Crosswhite, B. Dunn, *J. Opt. Soc. Am.* **1961**, *51*, 820 – 827.
[18] J.-C. G. Bünzli, C. Piguet, *Chem. Rev.* **2002**, *102*, 1897 – 1928.
[19] J.-C. G. Bünzli, C. Piguet, *Chem. Soc. Rev.* **2005**, *34*, 1048 – 1077.
[20] K. Binnemans in *Handbook on the Physics and Chemistry of Rare Earths,* Vol. 35 (Eds.: K. A. Gschneidner, Jr., J.-C. G. Bünzli, V. K. Pecharsky), Elsevier, Amsterdam, **2005**, chapter 225, pp. 107 – 272.
[21] M. Hilder, M. Lezhnina, M. L. Cole, C. M. Forsyth, P. C. Junk, U. H. Kynast, *J. Photochem. Photobiol., A* **2011**, *217*, 76 – 86.
[22] G. F. de Sa, O. L. Malta, C. de Mello Donegá, A. M. Simas, R. L. Longo, P. A. Santa-Cruz, E. F. da Silva, Jr., *Coord. Chem. Rev.* **2000**, *196*, 165 – 195.
[23] O. V. Kotova, S. V. Eliseeva, A. A. Volosnikov, V. A. Oleinikov, L. S. Lepnev, A. G. Vitukhnovskii, N. P. Kuzmina, *Russ. J. Coord. Chem.* **2006**, *32*, 901 – 909.
[24] T. H. Tran, M. M. Lezhnina, U. Kynast, *J. Mater. Chem.* **2011**, *21*, 12819 – 12823.
[25] Y. Hasegawa, M. Yamamuro, Y. Wada, N. Kanehisa, Y. Kai, S. Yanagida, *J. Phys. Chem. A* **2003**, *107*, 1697 – 1702.
[26] J. Kai, M. C. F. C. Felinto, L. A. O. Nunes, O. L. Malta, H. F. Brito, *J. Mater. Chem.* **2011**, *21*, 3796 – 3802.
[27] D. F. Parra, A. Mucciolo, H. F. Brito, L. C. Thompson, *J. Solid State Chem.* **2003**, *171*, 412 – 419.

[28] X. Wang, Q. Yan, P. Chu, Y. Luo, Z. Zhang, S. Wu, L. Wang, Q. Zhang, *J. Lumin.* **2011**, *131*, 1719 – 1723.
[29] P. L. Forster, D. F. Parra, J. Kai, D. M. Fermino, H. F. Brito, A. B. Lugao, *Radiat. Phys. Chem.* **2010**, *79*, 347 – 349.
[30] T. Fiedler, M. Hilder, P. C. Junk, U. H. Kynast, M. M. Lezhnina, M. Warzala, *Eur. J. Inorg. Chem.* **2007**, 291 – 301.
[31] M. Hilder, P. C. Junk, M. M. Lezhnina, M. Warzala, U. H. Kynast, *J. Alloys Compd.* **2008**, *451*, 530 – 533.
[32] R. Reisfeld, T. Saraidarov, G. Panzer, V. Levchenko, M. Gaft, *Opt. Mater.* **2011**, *34*, 351 – 354.
[33] X. Wu, L. Liu, W. Zhang, S. Hu, R. Jin, L. Zhang, *J. Rare Earths* **2006**, *24*, 61 – 63.
[34] V. V. Semenov, N. V. Zolotareva, V. N. Myakov, E. Y. Ladilina, E. V. Lapshina, M. A. Lopatin, I. Y. Ruskol, E. I. Alekseeva, S. R. Nanush'yan, *Russ. J. Gen. Chem.* **2012**, *82*, 1513 – 1516.
[35] H. L. Fang Xie, G. Zhong, F. Deng, *Optoelectr. Adv. Mater., Rapid Commun.* **2010**, *4*, 685 – 688.
[36] L. Van Meervelt, A. Froyen, W. D'Olieslager, C. Walrand-Görller, I. Drisque, G. S. D. King, S. Maes, A. T. H. Lenstra, *Bull. Soc. Chim. Belg.* **1996**, *105*, 377 – 381.
[37] J. G. Leipoldt, L. D. C. Bok, A. E. Laubscher, S. S. Basson, *J. Inorg. Nucl. Chem.* **1975**, *37*, 2477 – 2480.
[38] J. Lu, K. Yu, H. Wang, J. He, G. Cheng, C. Qin, J. Lin, W. Wei, B. Peng, *Opt. Mater.* **2008**, *30*, 1531 – 1537.
[39] R. G. Charles, R. C. Ohlmann, *J. Inorg. Nucl. Chem.* **1965**, *27*, 119 – 127.
[40] I. Diaz-Acosta, J. Baker, W. Cordes, P. Pulay, *J. Phys. Chem. A* **2000**, *105*, 238 – 244.
[41] A. Gleizes, S. Sans-Lenain, D. Medus, N. Hovnanian, P. Miele, J. D. Foulon, *Inorg. Chim. Acta* **1993**, *209*, 47 – 53.
[42] N. Filipescu, G. W. Mushrush, C. R. Hurt, N. McAvoy, *Nature* **1966**, 211, 960 – 961.
[43] T. H. Tran, M. Bentlage, M. M. Lezhnina, U. Kynast, *J. Photochem. Photobiol., A* **2014**, *273*, 43 – 48.
[44] L. N. Puntus, K. A. Lyssenko, I. S. Pekareva, J.-C. G. Bünzli, *J. Phys. Chem. B* **2009**, *113*, 9265 – 9277.